Inorg. Chem. **2003**, *42*, 3540–3548

Aggregate Manganese Schiff Base Moieties by Terephthalate or Acetate: Dinuclear Manganese and Trinuclear Mixed Metal Mn_2/Na Complexes

Changneng Chen,[†] Deguang Huang,[†] Xiaofeng Zhang,[†] Feng Chen,[†] Hongping Zhu,[†] Qiutian Liu,*[,†] Cunxi Zhang,[‡] Daizheng Liao,[§] Licun Li,[§] and Licheng Sun[||]

State Key Laboratory of Structural Chemistry, Fujian Institute of Research on the Structure of Matter, Chinese Academy of Sciences, Fuzhou, Fujian 350002, China, Department of Biochemistry, Center for Chemistry and Chemical Engineering, Lund University, 124, 221 00 Lund, Sweden, Department of Chemistry, Nankai University, Tianjing 300071, China, and State Key Laboratory of Fine Chemicals, Dalian University of Technology, Dalian, China

Received August 9, 2002

A reaction system consisting of terephthalic acid, NaOH, inorganic Mn(II) or Mn(III) salt, and salicylidene alkylimine resulted in dinuclear manganese complexes $(salpn)_2Mn_2(\mu\text{-phth})(CH_3OH)_2$ (**1**, salpn = *N*,*N*′-1,3-propylene-bis(salicylideneiminato); phth = terephthalate dianion), $(salen)_2Mn_2(\mu\text{-phth})(CH_3OH)_2$ (**2**, salen = *N*,*N*′-ethylene-bis(salicylideneiminato)), $(salen)_2Mn_2(\mu\text{-phth})(CH_3OH)(H_2O)$ (**3**), and $(salen)_2Mn_2(\mu\text{-phth})$ (**4**), while the absence of NaOH in the reaction led to a mononuclear Mn complex $(salph)Mn(CH_3OH)(NO_3)$ (**5**, salph = *N*,*N*′-1,2-phenylene-bis(salicylideneiminato)). In addition, a trinuclear mixed metal complex $H\{Mn_2Na(salpn)_2(\mu\text{-OAc})_2(H_2O)_2\}(OAc)_2$ (**6**) was obtained from the reaction system by using maleic acid instead of terephthalic acid. Five-coordinate Mn ions were found in **4** giving rise to an intermolecular interaction and constructing a one-dimensional linear structure. Antiferromagnetic exchange interactions were observed for **1**–**3**, and a total ferromagnetic exchange of **4** was considered to stem from intermolecular magnetic coupling. ^1H NMR signals of phenolate ring and alkylene (or phenylene) backbone of the diamine are similar to those reported in the literature, and the phth protons are at –2.3 to –10.1 ppm. Studies on structure, bond valence sum analysis, and magnetic properties indicate the oxidation states of the Mn ions in **6** to be +3, which are also indicated by ESR spectra in dual mode. Ferromagnetic exchange interaction between the Mn(III) sites was observed with $J = 1.74\ cm^{-1}$. A quasireversible redox pair at –0.29V/–0.12V has been assigned to the redox of Mn_2(III)/Mn(III)Mn(II), implying the intactness of the complex backbone in solution.

Introduction

Various intricate structures organized from simple units have been found in biological systems. Chemists are challenged to assemble the specific structures from metal building blocks for simulating the biological cluster. Manganese complexes have attracted considerable interest in recent years because of their presence in various biosystems,[1] especially in the oxygen-evolving complex (OEC) of photosystem II (PSII). Dinuclear manganese complexes have been reported for water oxidation to generate dioxygen[2] and have been used to artificially model[3] PSII. Several 4Mn models[4] for the oxygen-evolving process during photosynthesis seem to hint that there are two Mn ions directly involved in the water oxidation, even though the tetranuclear Mn cluster[5] has been

* To whom correspondence should be addressed. E-mail: lqt@ms.fjirsm.ac.cn.
[†] Fujian Institute.
[‡] Lund University.
[§] Nankai University.
[||] Dalian University of Technology.

(1) (a) Law, N. A.; Caudle, M. T.; Pecoraro, V. L. *Adv. Inorg. Chem.* **1998**, *46*, 305. (b) Yachandra, V. K.; Sauer, K.; Klein, M. P. *Chem. Rev.* **1996**, *96*, 2927. (c) Tommos, C.; Babcook, G. T. *Acc. Chem. Rev.* **1998**, *31*, 18.
(2) (a) Ashmawy, F. W.; McAuliffe, C. A.; Parish, R. V.; Tames, J. *J. Chem. Soc., Dalton Trans.* **1985**, 1391. (b) Limburg, J.; Vrettos, J. S.; Liable-Sands, L. M.; Rheingold, A. L.; Crabtree, R. H.; Brudvig, G. W. *Science* **1999**, *283*, 1524.
(3) Sun, L.; Raymond, M. K.; Magnuson, A.; LeGourriérec, D.; Tamm, M.; Abrahamsson, M.; Kenéz, P. H.; Mårtensson, J.; Stenhagen, G.; Hammarström, L.; Styring, S.; Åkermark, B. *J. Inorg. Biochem.* **2000**, *78*, 15.

10.1021/ic025944z CCC: $25.00
Published on Web 04/29/2003

proved to exist in the OEC of PSII. Manganese (II and III) ions have been suggested to locate in the terminal position of the 4Mn models in S_0 state[6] as the aqua binding site(s).[4] However, the unknown structure of the Mn sites in the OEC has stimulated extensive imagination for chemists and promoted the preparation of discrete Mn units and the rational design of aggregating the units to access the OEC structure. A polydentate Schiff base, such as salicylidene alkylimine, has been often used to construct the Mn unit with an N/O coordination sphere. Several dinuclear and polynuclear Mn complexes have been assembled[7] from these Mn/Schiff base units by carboxyl, oxo, or cyano bridges, of which dicarboxylate[7,8] as one of the bridges behaves as either a dianion or a monoanion to link the Mn units. We are interested in the formation of the dinuclear manganese complexes in the presence of dicarboxylic acid,[9] since this assembly may have some potential interest for the aggregate of the manganese unit, leading to a polynuclear Mn cluster relevant to the biosystem. Meanwhile, bimetal model complexes containing Mn and a redox-inactive metal have also been attractive,[10,11] because a strict calcium requirement[12] has been known for the component and the function of the OEC. In this paper, our efforts using the phth dianion to assemble the Mn/Schiff base units are reported. Four new Mn_2 complexes containing the phth dianion bridge are presented. Also included in this paper is a bimetal trinuclear Mn_2/Na complex, in which the Mn/Schiff base units are linked through a sodium ion and acetates.

Experimental Section

All manipulations were performed under aerobic conditions with materials as received. The Schiff base was obtained from a reaction of salicylaldehyde with diamine ($NH_2CH_2CH_2NH_2$, $NH_2CH_2CH_2CH_2NH_2$, and *o*-phenylenediamine).

[(salpn)$_2$Mn$_2$(μ-phth)(CH$_3$OH)$_2$]·2H$_2$O (1·2H$_2$O). Terephthalic acid (0.41 g, 2.47 mmol) and NaOH (0.20 g, 5.00 mmol) were added in 20 mL of CH_3OH/H_2O (v/v 1:1) and stirred for 0.5 h. To the solution were successively added $Mn(OAc)_2·2H_2O$ (0.43 g, 1.60 mmol) and H_2salpn (0.58 g, 2.05 mmol), and the solution was stirred at room temperature for 2 h, resulting in dark green precipitates, which were collected by filtration. The precipitates were purified by recrystallization in CH_3OH to get 0.36 g (yield 48.1%) of black needle crystals. Anal. Calcd for **1**·2H$_2$O, $C_{44}H_{48}Mn_2N_4O_{12}$: C, 56.53; H, 5.14; Mn, 11.76; N, 5.99. Found: C, 56.55; H, 5.23; Mn, 11.38; N, 5.80.

[(salpn)$_2$Mn$_2${μ-*p*-C$_6$D$_4$(COO)$_2$}(CH$_3$OH)$_2$]·2H$_2$O (D1·2H$_2$O). The preceding procedure was performed in a very small scale with a proportional reduction of the reactants of which deuterated terephthalic acid was used instead of terephthalic acid. Crystals obtained were identified by X-ray diffraction.

[(salen)$_2$Mn$_2$(μ-phth)(CH$_3$OH)$_2$]·4H$_2$O (2·4H$_2$O). The synthetic procedure of **1**·2H$_2$O was utilized to synthesize **2**·4H$_2$O (0.40 g, yield 42.5%) with the use of H_2salen instead of H_2salpn. Anal. Calcd for **2**·4H$_2$O, $C_{42}H_{48}Mn_2N_4O_{14}$: C, 53.50; H, 5.12; Mn, 11.65; N, 5.94. Found: C, 53.67; H, 4.91; Mn, 12.4; N, 6.02.

[(salen)$_2$Mn$_2$(μ-phth)(CH$_3$OH)(H$_2$O)]·3H$_2$O (3·3H$_2$O). Terephthalic acid (0.25 g, 1.51 mmol) and NaOH (0.12 g, 3.00 mmol) were added in 25 mL of CH_3OH/H_2O (v/v 1:1) solution and stirred for 1 h. To the solution was added $Mn(OAc)_3·2H_2O$ (0.268 g, 1.00 mmol), and the mixture was stirred for 5 h. Then, a solution of H_2salen (0.268 g, 1.00 mmol) in 15 mL of CH_3CN was successively added, and the solution was refluxed under stirring for 5 h. After cooling and filtration, the filtrate was allowed to stand for a week, resulting in black red crystals, which were collected by filtration to afford 0.20 g (yield 43.4%) of **3**·3H$_2$O. Anal. Calcd for **3**·3H$_2$O, $C_{41}H_{44}Mn_2N_4O_{13}$: C, 54.07; H, 4.87; N, 6.15. Found: C, 53.36; H, 4.13; N, 5.99.

[(salen)$_2$Mn$_2${μ-*p*-C$_6$D$_4$(COO)$_2$}(CH$_3$OH)(H$_2$O)]·3H$_2$O (D3·3H$_2$O). The preceding procedure for **3**·3H$_2$O was performed in a very small scale with a proportional reduction of the reactants of which deuterated terephthalic acid was used instead of terephthalic acid. Crystals obtained were identified by X-ray diffraction.

[(salen)$_2$Mn$_2$(μ-phth)]·2CH$_3$OH (4·2CH$_3$OH). Terephthalic acid (0.415 g, 2.50 mmol) and NaOH (0.20 g, 5.00 mmol) were added to 20 mL of CH_3OH/H_2O (v/v 1:1), and the reaction mixture stirred for 1 h. To the solution was added manganese(III) acetylacetonate (0.70 g, 1.99 mmol), and the mixture was stirred for 2 h. Then, a solution of H_2salen (0.536 g, 2.00 mmol) and Et_4NBr (0.42 g, 2.0 mmol) in 15 mL of CH_3CN was successively added, and the solution was stirred for 1.5 h. After filtration, the filtrate and the precipitates were treated, respectively, in the following ways. From the filtrate, **2**·4H$_2$O was isolated. The precipitates were dissolved in 15 mL of CH_3OH and filtered to remove the undissolved residue. The filtrate was allowed to stand for 3 days, resulting in black red crystals, which were collected by filtration to afford 0.32 g (yield 36.8%) of **4**·2CH$_3$OH. Anal. Calcd for **4**·2CH$_3$OH, $C_{42}H_{40}Mn_2N_4O_{10}$: C, 57.93; H, 4.63; N, 6.44. Found: C, 57.08; H, 4.29; N, 6.42.

(salph)Mn(CH$_3$OH)(NO$_3$)·CH$_3$CN (5·CH$_3$CN). Terephthalic acid (0.41 g, 2.47 mmol) and H_2salph (2 mmol) were added to 30 mL of CH_3OH/H_2O (v/v 1:1) and stirred for 1 h. Then, $Mn(NO)_3·4H_2O$ (0.64 g, 2.55 mmol) was added and stirred for 2 h at 50 °C. After filtration, the filtrate was allowed to stand for several days to deposit black crystals, which were collected, and dried in vacuo, affording 0.15 g (yield 16% based on H_2salph) of **5**·CH$_3$CN. Anal.

(4) (a) Hoganson, C. W.; Babcock, G. T. *Science* **1997**, *277*, 1953. (b) Peloquin, J. M.; Campbell, K. A.; Randall, D. W.; Evanchik, M. A.; Pecoraro, V. L.; Armstrong, W. H.; Britt, R. D. *J. Am. Chem. Soc.* **2000**, *122*, 10926. (c) Zhang, C.-X.; Pan, J.; Li, L.-B.; Kuang, T.-Y. *Chin. Sci. Bull* **1999**, *44*, 2209.

(5) Zouni, A.; Witt, H. T.; Kern, J.; Fromme, P.; Krauss, N.; Saenger, W.; Orth, P. *Nature* **2001**, *409*, 739.

(6) Iuzzolino, L.; Dittmer, J.; Döyner, W.; Meyer-Klaucke, W.; Dau, H. *Biochemistry* **1998**, *37*, 17112.

(7) (a) Bonadies, J. A.; Kirk, M. L.; Lah, M. S.; Kessissoglou, D. P.; Hatfield, W. E.; Pecoraro, V. L. *Inorg. Chem.* **1989**, *28*, 2037. (b) Zhang, Z. Y.; Brouca-Cabarrecq, C.; Hemmert, C.; Dahan, F.; Tuchagues, J. P. *J. Chem. Soc., Dalton Trans.* **1995**, 1453. (c) Bermejo, M. R.; Fondo, M.; García-Deibe, A.; González, A. M.; Sousa, A.; Sanmartín, J.; McAuliffe, C. A.; Pritchard, R. G.; Watkinson, M.; Lukov, V. *Inorg. Chim. Acta* **1999**, *293*, 210. (d) Horner, O.; Anxolabéhère-Mallart, E.; Charlot, M.; Tchertanov, L.; Guilhem, J.; Mattioli, T. A.; Boussac, A.; Girerd, J. *Inorg. Chem.* **1999**, *38*, 1222. (e) Matsumoto, N.; Sunatsuki, Y.; Miyasaka, H.; Hashimoto, Y.; Luneau, D.; Tuchagues, J. P. *Angew. Chem., Int. Ed.* **1999**, *38*, 171.

(8) (a) Wemple, M. W.; Tsai, H. L.; Wang, S.; Claude, J. P.; Streib, W. E.; Huffman, J. C.; Hendrickson, D. N.; Christou, G. *Inorg. Chem.* **1996**, *35*, 6437. (b) Cano, J.; de Munno, G.; Sanz, J. L.; Ruiz, R.; Faus, J.; Lloret, F.; Julve, M.; Caneschi, A. *J. Chem. Soc., Dalton Trans.* **1997**, 1915. (c) Xiang, S. T.; Jie, S.; Dao, F. X.; Wen, X. T. *Inorg. Chim. Acta* **1997**, *255*, 157. (d) Cano, J.; de Munno, G.; Sanz, J.; Ruiz, R.; Lloret, F.; Faus, J.; Julve, M. *J. Chem. Soc., Dalton Trans.* **1994**, 3465.

(9) Chen, C.; Zhu, H.; Huang, D.; Wen, T.; Liu, Q.; Liao, D.; Cui, J. *Inorg. Chim. Acta* **2001**, *320*, 159.

(10) Reynolds, R. A.; Coucouvanis, D. *J. Am. Chem. Soc.* **1998**, *120*, 209.

(11) Bonadies, J. A.; Kirk, M. L.; Lah, M. S.; Kessissoglou, D. P.; Hatfield, W. M.; Pecoraro, V. L. *Inorg. Chem.* **1989**, *28*, 2037.

(12) Yocum, C. F. *Manganese Redox Enzymes*; Pecoraro, V. L., Ed.; VCH: New York, 1992; p 71.

Table 1. Crystallographic Data for Complexes **1**−**6**, **D1**, and **D3**

complex	**1**·2H_2O	**D1**·2H_2O	**2**·4H_2O	**3**·3H_2O	**D3**·3H_2O	**4**·2CH_3OH	**5**·CH_3CN	**6**·2CH_3OH
formula	$C_{44}H_{48}Mn_2N_4O_{12}$	$C_{44}H_{44}D_4Mn_2N_4O_{12}$	$C_{42}H_{48}Mn_2N_4O_{14}$	$C_{41}H_{44}Mn_2N_4O_{13}$	$C_{41}H_{40}D_4Mn_2N_4O_{13}$	$C_{42}H_{40}Mn_2N_4O_{10}$	$C_{21}H_{18}MnN_3O_6$	$C_{44}H_{57}Mn_2N_4NaO_{16}$
fw	934.74	938.75	942.72	910.68	914.69	870.66	463.33	1030.81
λ(Mo Kα)	0.71073	0.71073	0.71073	0.71073	0.71073	0.71073	0.71069	0.71073
T, °C	20	20	20	20	20	20	20	20
space group	$P2_1/n$	$P2_1/n$	$P2_1/c$	$P2_1$	$P2_1$	$P\bar{1}$	$P2_1/c$	$P\bar{1}$
a, Å	11.144(2)	11.1508(14)	7.5982(5)	7.5982(1)	7.6286(3)	9.7564(9)	9.957(2)	9.4766(19)
b, Å	10.878(2)	10.8604(12)	12.5587(9)	12.3969(3)	12.4571(5)	10.056(1)	7.868(2)	10.345(2)
c, Å	18.917(4)	18.883(2)	22.5905(16)	20.9815(5)	21.0959(8)	11.7627(11)	25.339(5)	12.618(3)
α, deg						84.565(1)		90.35(3)
β, deg	100.30(3)	100.098(2)	95.519(1)	90.34(2)	90.228(2)	65.629(2)	95.53(3)	105.87(3)
γ, deg						65.984(2)		92.34(3)
V, Å^3	2256.3(8)	2251.4(5)	2145.7(3)	1976.30(7)	2004.73(14)	956.48(16)	1975.9(7)	1188.7(4)
Z	2	2	2	2	2	1	4	1
ρ_{calcd}, g/cm^3	1.376	1.373	1.459	1.515	1.502	1.491	1.554	1.440
μ, mm^{-1}	0.624	0.625	0.661	0.712	0.702	0.726	0.714	0.614
R^a	0.0655	0.0949	0.0592	0.0522	0.0586	0.0838	0.0442	0.0621
$R_w{}^b$	0.1859	0.1852	0.1542	0.1369	0.1253	0.1898	0.1319	0.1635

^{a} $R = \sum||F_o| - |F_c||/\sum|F_o|$. ^{b} $R_w = [\sum w(|F_o| - |F_c|)^2/\sum wF_o^2]^{1/2}$. $w = 1/[S^2(F_o^2) + (0.1000P)^2 + 0.0000P]$ for **1**−**6**, $w = 1/[S^2(F_o^2) + (0.0502P)^2 + 5.3792P]$ for **D1**, and $w = 1/[S^2(F_o^2) + (0.0717P)^2 + 6.7596P]$ for **D3**. $P = (F_o^2 + 2F_c^2)/3$.

Calcd for $C_{21}H_{18}MnN_3O_6$: C, 54.44; H, 3.92; N, 9.07. Found: C, 54.74; H, 3.28; N, 9.24.

[H{$Mn_2Na(salpn)_2(\mu$-OAc)$_2(H_2O)_2$}(OAc)$_2$]·2CH_3OH (6·2CH_3OH). A 0.29 g (2.5 mmol) portion of maleic acid and 0.20 g (5 mmol) of NaOH were combined in a mixed solvent (H_2O/CH_3OH, 10/10 mL), and the solution was stirred for 0.5 h. Then, a solution of 0.43 g (1.6 mmol) of $Mn(OAc)_3·2H_2O$ in 20 mL of CH_3CN and 0.58 g (2.05 mmol) of H_2salpn were added and stirred for 13 h at room temperature. After filtration, the filtrate was concentrated in vacuo to dryness, and the residue was dissolved in CH_3OH and filtered to obtain a brown filtrate, which was volatilized naturally to deposit rectangle crystals, affording 0.14 g (yield 17.0%) of the complex. Anal. Calcd for **6**·2CH_3OH: C, 51.26; H, 5.57; Mn, 10.66; N, 5.44. Found: C, 51.65; H, 5.37; Mn, 10.59; N, 5.43.

X-ray Structure Determination. All the crystals suitable for X-ray diffraction were selected from the reaction solutions. The diffraction data were collected on a Siemens SMART CCD diffractometer with graphite monochromated Mo Kα radiation (λ = 0.71073 Å) using the ω-scan mode at 293 K for **2**, **3**, **4**, **D1**, and **D3**, an Enraf Nonius CAD4 diffractometer for **1**, and an AFC5R Rigaku diffractometer for **5** and **6**. The intensity data were corrected for Lorentz-polarization factors, and empirical absorption correction was applied. The structures were solved by direct methods and Fourier techniques for each compound and refined by full-matrix least-squares calculation with the SHELXL-97 program package.[13] All the non-hydrogen atoms were refined anisotropically except for the oxygen atoms in the solvate H_2O of complexes **1** and **D1**, which were statistically distributed in three positions with identical occupancy. Two atoms in counterion AcO^- for complex **6** were found to be disordered in two positions with respective occupancy of 0.5 and to be considered as C′ (C″) and O′ (O″) atoms. The other assumption of $(CH_3)_2CO$ instead of the counterion AcO^- seems to also give a rational refinement. However, no acetone was included in the procedures of the synthesis and the crystallization of **6**, so the acetone molecules were excluded in the structure. For all complexes, hydrogen atoms were geometrically located and added to the structure factor calculations, but their positions were not refined. The deuterium atoms in **D1** and **D3** were treated as hydrogen atoms. The crystallographic data were compiled in Table 1.

(13) SHELXTL: *SAINT and SHELXTL (Version 5.0)*; Siemens Analytical X-ray Instruments Inc.: Madison, WI, 1994.

Other Physical Measurements. IR spectra were recorded on a Magna-75-FT-IR spectrophotometer as KBr pellets (4000−400 cm^{-1}). The ^{1}H NMR spectra were recorded on a Bruker-AM 500 spectrometer with TMS as standard. The EPR spectra were recorded on a Bruker-ER420 spectrometer at room temperature and 77 K for solid samples. The further EPR determination was performed in dual mode on a Bruker 380E spectrometer. The sample (2.0 mM) dissoved in H_2O/CH_3OH (v/v 1/4) was filled into a calibrated quartz EPR tube, then frozen in liquid nitrogen (77 K). The background was measured on the same solvent without the sample and was deducted from the sample spectrum. Continuous-wave EPR spectra were recorded with one Bruker ER4116DM dual mode cavity capable of either perpendicular or parallel polarization of the applied magnetic field. The cryogenic temperature was obtained with an Oxford ESR900 liquid helium cryostat. An Oxford ITC503 temperature and gas flow controller was used to control the temperature. The variable temperature susceptibility was measured on a model CF-1 superconducting magnetometer with a crystalline sample kept in a capsule at 5−300 K. Diamagnetic corrections were made with Pascal's constants for all the constituent atoms of the complexes determined. The electrochemical measurement was performed in the cyclic voltammetric mode on a CV-1B cyclic voltammeter in CH_3OH with an SCE reference electrode, graphite working electrode, and Pt auxiliary electrode. The supporting electrolyte was Et_4NBF_4. Elemental analyses were performed by Germany Elemental Analyzer Vario EL III.

Results and Discussion

Synthesis. In complexes **1**−**4**, two Mn/N_2O_2 Schiff base subunits are connected by the phth dianion. Sodium hydrate must be first used in the synthetic procedure to produce the phth dianion and to lead to the formation of the Mn−$OCOC_6H_4COO$−Mn skeleton. The final participation of the N_2O_2 Schiff base results in the dinuclear Mn complexes **1**−**4**. Otherwise, if the N_2O_2 Schiff base first reacts with the Mn salt to form the Mn/N_2O_2 Schiff base intermediate or mononuclear Mn complex such as **5**, both the Mn intermediates will be difficult to combine with each other by the phth dianion. So, a strong alkali environment would be important for the formation of the dinuclear Mn complexes. Meanwhile, the use of maleic acid in the reaction system instead of

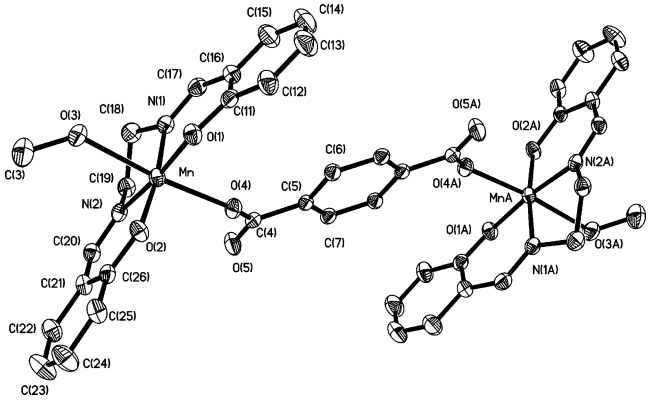

Figure 1. Structure of **2** with selected atom-labeling, showing the thermal ellipsoids of 30% probability surfaces.

Table 2. Selected Bond Lengths (Å) for Complexes **1**−**4**

	1	**2**	**3**	**4**
Mn−O1	1.886(3)	1.875(3)	1.895(4), 1.877(4)	1.865(4)
Mn−O2	1.882(3)	1.885(3)	1.872(4), 1.879(4)	1.893(4)
Mn−N1	2.033(4)	1.981(3)	1.995(5), 1.975(5)	1.979(5)
Mn−N2	2.034(4)	1.976(4)	1.967(5), 1.963(5)	1.969(5)
Mn−O4 (COO)	2.102(3)	2.197(3)	2.215(5), 2.182(5)	2.084(4)
Mn−O3 (CH_3OH)	2.338(4)	2.291(4)	2.291(5)	
			2.247(5) (H_2O)	

terephthalic acid leads to a different result in that trinuclear Mn_2Na complex **6** was separated. It is proposed that the stereo effect of both the carboxylic groups in maleic acid may not be favorable to link both the Mn/N_2O_2 Schiff base moieties. However, the preparation of **6** is repeatable in low yield (ca. 15%) in the participation of maleic acid. Other unseparated product in the reaction system remains to be studied.

Structure. Complexes **1**, **2**, and **3** possess an almost identical molecule structure. The molecule structures of **1** and **2** result from two half units, which are related by a crystallographic center located at the center of the benzene ring of the phth. Figure 1 shows the structure of **2** as the representative of the three complexes. Deuterated complexes **D1** and **D3** have the same structures as those of **1** and **3**, respectively.

The Mn ions are six-coordinate with four N_2O_2 donor atoms of salen or salpn located at an equatorial plane of a distorted octahedron with trans angles O−Mn−N ranging from 171.40(14)° to 175.92(14)°. In addition, both oxygen donor atoms from the μ-phth bridge and the terminal ligand (CH_3OH or H_2O) completed the fifth and sixth coordinations with the trans angle range 171.62(17)°−179.1(2)°. The $Mn-O_{carboxyl}$ (2.102(3)−2.197(3) Å) and the $Mn-O_{terminal}$ (2.247(5)−2.338(4) Å) are obviously lengthened (Table 2) indicating the evidence for a Jahn−Teller elongation of Mn^{III} with high spin d^4 along the axial direction. In contrast with the six-coordinate Mn sites in **1**−**3**, the Mn atoms in **4** are five-coordinate with an approximate square pyramid sphere. The N_2O_2 donors are at the basal plane, and the carboxylic O atom is at the apical position with $O_{apical}-Mn-N(O)$ angles ranging from 92.62(19)° to 99.12(19)° and other O−Mn−N angles ranging from 165.8(2)° to 167.56(19)°. Both the Mn/N_2O_2 moieties are bridged by phth in the same mode as that in **1**−**3** as shown in Figure 2. It is interesting

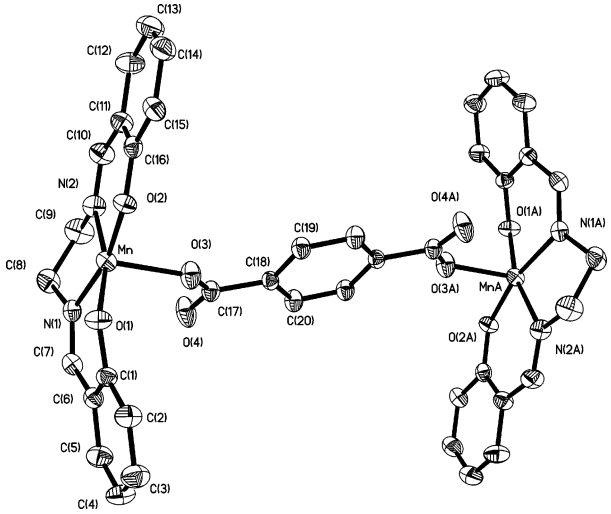

Figure 2. Structure of **4** with selected atom-labeling, showing the thermal ellipsoids of 30% probability surfaces.

that the five-coordinate Mn/N_2O_2 moieties of adjacent molecules are correlated by a $Mn\cdots O_{phenolate}$ separation of 2.773 Å, which is shorter than the sum of the van der Waals radii of the Mn and the O atoms, implying weak interaction between the molecules. Consequently, an intermolecular Mn···Mn separation of 3.564 Å was observed to be the shortest metallic separation in comparison with the intramolecular ones. Complex **4** can be considered to have a one-dimensional linear structure as shown in Figure 3, if the intermolecular Mn···O separation is assumed as the sixth coordination bond of the Mn atom.

In these complexes, the existence of solvate water or CH_3OH molecules gives rise to hydrogen bonding interactions. The solvate molecules are hydrogen bonded to the carboxylic and phenolate groups, as well as methanol or aqua ligands. These hydrogen bonds connect the neighboring molecules forming a supramolecular structure for complexes **1**−**3**. However, the hydrogen bonds in complex **4** seem not to be important as the hydrogen bonds do not result in any connection between the chains.

The molecular structure of complex **5** is illustrated in Figure 4. The coordination geometry of the Mn ion can be described as a distorted octahedron. The bond distances and angles in the $Mn(N_2O_2)$ unit are normal for a Mn(III) Schiff base complex. Jahn−Teller elongation along the axial direction is also observed with Mn−O3 and Mn−O6 distances of 2.336(3) and 2.329(2) Å, respectively. However, the trans angle O3−Mn−O6 of 162.06(9)° is obviously deviating from 180°. Selected bond distances are listed in Table 3 falling into the common range of other (salph)Mn(III) complexes.[14]

Figure 5 shows the structure of **6** which is composed of two crystallgraphically equivalent Mn(salpn) moieties and a Na^+ ion locating on a crystallographic inversion center with

(14) (a) McAuliffe, C. A.; Nabhan, A.; Pritchard, R. G.; Watkinson, M.; Bermejo, M.; Sousa, A. *Acta Crystallogr.* **1994**, *C50*, 1676. (b) Fukuda, T.; Sakamoto, F.; Sato, M.; Nakano, Y.; Tan, X. S.; Fujii, Y. *Chem. Commun.* **1998**, 1391. (c) Li, J.; Yang, S.-M.; Zhang, F.-X.; Tang, Z.-X.; Shi, Q.-Z.; Wu, Q.-J.; Huang, Z.-X. *Chin. J. Inorg. Chem.* **2000**, *16*, 84.

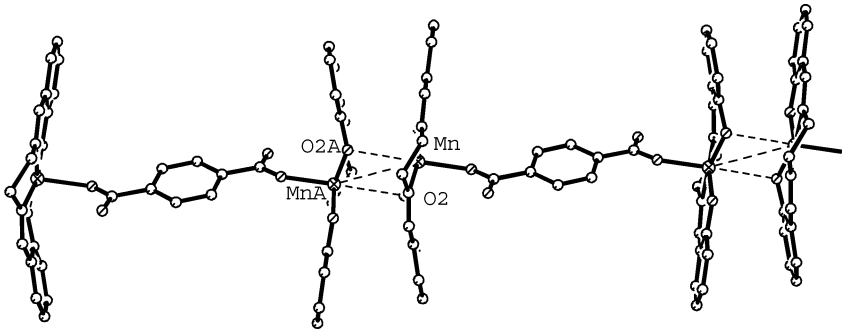

Figure 3. View of the packing drawing of **4** showing the one-dimensional chain structure with the intramolecular Mn···Mn separation of 11.390 Å. The dashed lines (- - -) indicate Mn···O, Mn···Mn, and hydrogen bonding interactions (Å): Mn···O2A, 2.773; Mn···MnA, 3.564; O0···O1, 3.068; O0···O2, 3.173. The oxygen atom O0 belongs to solvate CH_3OH (omitted).

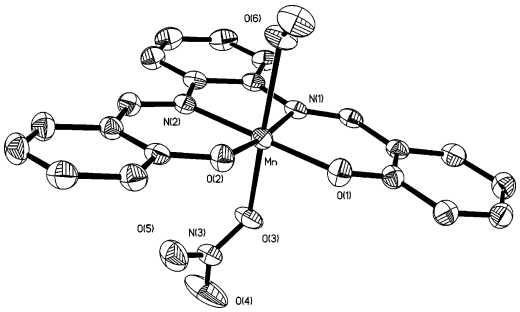

Figure 4. Structure of **5** with selected atom-labeling, showing the thermal ellipsoids of 30% probability surfaces.

Table 3. Selected Bond Lengths (Å) for Complex **5**

Mn−O1	1.850(2)	Mn−O2	1.875(2)
Mn−N1	1.990(3)	Mn−N2	1.986 (3)
Mn−O3	2.336(3)	Mn−O6	2. 329(2)

Mn····Na separation of 3.2717(11) Å. Three octahedrally distorted metal ions are linked by acetato and phenolato bridges. Selected bond distances of **6** are listed in Table 4. Bond angles around the Mn ion are close to those requested for a octahedron with the trans angles of ca. 174° and the other angles ranging from 86.70(15)° to 96.11(13)°. The trans configuration of the trinuclear cluster exhibits the structural similarity of the backbones in complex **6** to that of a reported Mn_2Na complex, $[C_2H_9O_2][Mn_2Na(2\text{-HO-salpn})_2(OAc)_4]$.[11] A proton was considered to locate in the inversion center between both symmetrically related acetate counterions to balance the charge, leading to a reasonable Mn(III) oxidation state for both the Mn ions, as illustrated in a packing diagram (Figure 6) in which O′···O′A separation of 3.2 Å shows a weak interaction between O′···H^+···O′A. The bond distances are characteristic of Jahn−Teller elongated Mn(III) ions along the O_{water}−Mn−$O_{carboxyl}$ direction, and all the structural parameters are comparable to those of the Mn_2(III)Na cluster $[C_2H_9O_2][Mn_2Na(2\text{-HO-salpn})_2(OAc)_4]$,[11] in which a proton was considered to locate between both solvate CH_3OH molecules to form a $[C_2H_9O_2]^+$ cation to balance the charge. In order to verify the assignment of the oxidation states for the Mn ions, bond valence sum (BVS) analysis[15] of metal−ligand bond lengths has been used. We calculate the BVS of the Mn sites in complex **6** according to eq 1

$$s = \exp[(r_0 - r)/B] \qquad (1)$$

where s and r are bond valence and the observed bond distance, respectively, and r_0 and B are empirically determined parameters obtained from the literature.[15b] The calculation of the BVS for the Mn sites in **6** is based on Mn−O bonds of 1.904, 1.897, 2.147, and 2.269 Å and Mn−N bonds of 2.028 and 2.036 Å. The r_0 values are 1.760 and 1.832 Å for Mn−O and Mn−N bonds, respectively, and B is 0.37.[15] The bond valences are calculated for each of these bonds by eq 1 and summed to give a BVS of 3.14 for both the Mn sites in complex **6**. The BVS value is very consistent with the evaluation of Mn(III) and supports that the compound contains two equivalent Mn(III) ions. However, further discussion for the valence of the Mn ions is necessary by using other characteristic methods (vide infra).

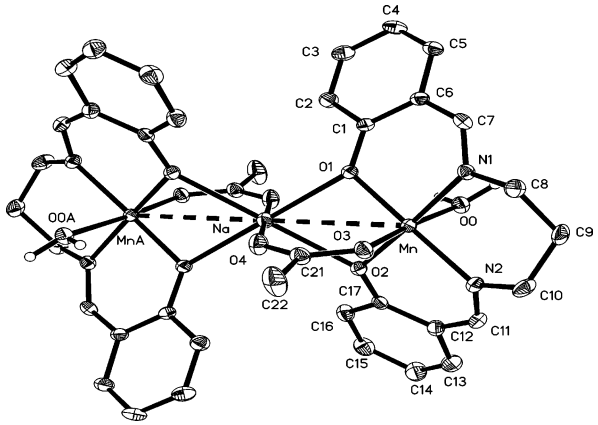

Figure 5. ORTEP diagram of the backbone $\{Mn_2Na(salpn)_2(\mu\text{-}OAc)_2(H_2O)_2\}^+$ in complex **6**, showing the thermal ellipsoids of 30% probability surfaces.

Table 4. Selected Bond Lengths (Å) for Complex **6**

Mn−O1	1.904(3)	Mn−O2	1.897(3)
Mn−N1	2.028(4)	Mn−N2	2.036(4)
Mn−O3	2.147(3)	Mn−O0	2.269(3)
Na−O1	2.336(3)	Na−O2	2.390(3)
Na−O4	2.402(3)	Na−Mn	3.2717(11)

^{1}H NMR Spectra of Complexes. Few of the ^{1}H NMR spectra were reported in the literature[16] for the Mn Schiff base complexes. Considering that (salen)Mn or (salpn)Mn is a relatively independent unit in the present compounds,

(15) (a) Thorp, H. H. *Inorg. Chem.* **1992**, *31*, 1585. (b) Brown, I. D.; Altermatt, D. *Acta Crystallogr.* **1985**, *B41*, 244.

(16) (a) Bonadies, J. A.; Maroney, M. J.; Pecoraro, V. L. *Inorg. Chem.* **1989**, *28*, 2044. (b) Li, X.; Pecoraro, V. L. *Inorg. Chem.* **1989**, *28*, 3403. (c) Larson, E. J.; Pecoraro, V. L. *J. Am. Chem. Soc.* **1991**, *113*, 3810.

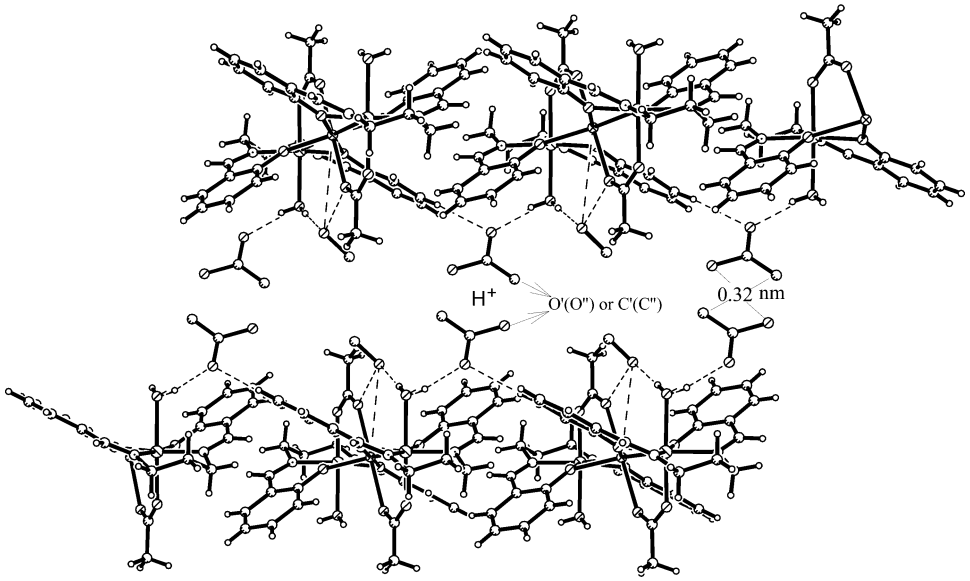

Figure 6. Packing diagram of complex **6**. Hydrogen bonding interactions are shown in dashed lines (- - -) between coordinated water and solvate CH_3OH molecules and acetate counterion. The disorders of the C′(C″) and O′(O″) atoms in the acetate and a proton locating at the inversion center for charge balance are described in the text.

complexes **1**−**6** could have analogous behavior with referred mononuclear compounds, such as (salen)MnCl (**7**).[16a] Figure 7 and Table 5 give the spectra and the assignments of related protons on the basis of comparison with reported data.

We have also observed several peaks which have not been reported or assigned. A broad resonance at −95 ppm occurs in the spectra of complexes **1** and **6**, though similar upfield signals for other dinuclear complexes **2**, **3**, and **4** were not observed because of too weak signal intensity arising from low solubility of the complexes in CD_3OD. The spectrum of (salen)MnCl (**7**)[16a] in Figure 7 contains the upfield signal at −122 ppm, implying the signal comes from the salen ligand. We tentatively assign the upfield signal to the contribution of 3-H in the phenol ring. It is interesting that several weak and broad peaks occur in the range from −2 to −10 ppm for complexes **1**−**4**, which contain a phth bridge different from that of other complexes. The peaks are assigned to the protons of the phth on the basis of the examination of the ^{1}H NMR spectra of structurally corresponding deuterated complexes **D1** and **D3**. The spectra of **D1** and **D3** exhibit the same features to those of **1** and **3**, respectively, except for the lack of the signals at the area (−2 to −10 ppm). This is also an indication that all these complexes maintain their backbone (salen)Mn−(μ-phth)−Mn(salen) or (salpn)Mn−(μ-phth)−Mn(salpn) in solution.

Magnetic Properties. Complexes **1**−**3** have identical backbones in the structures and are expected to have the same magnetic properties. The magnetic properties of **1** and **2** are discussed here and illustrated as the temperature dependence of the effective magnetic moment (μ_{eff}) values and molar susceptibility (χ_M) values in Figure 8. At room temperature, their μ_{eff} values amount to 6.92 and 7.03 μ_B, which are close to the value expected for two independent spins $S = 2$ (6.92 μ_B). With the temperature decreases in the range 300−30 K, the μ_{eff} value slightly decreases and then rapidly decreases. Because the phth bridge results in a long Mn···Mn separation, it is believed that the two Mn(III) ions undergo only weak magnetic exchange interaction with the exchange integral J. The following eq 2 was used for calculating the susceptibilities of **1** and **2**.

$$\chi = \frac{2Ng^2\beta^2}{kT}\left[\frac{A}{B}\right] \qquad (2)$$

$$A = 30 + 14\exp\left(\frac{-8J}{kT}\right) + 5\exp\left(\frac{-14J}{kT}\right) + \exp\left(\frac{-18J}{kT}\right)$$

$$B = 9 + 7\exp\left(\frac{-8J}{kT}\right) + 5\exp\left(\frac{-14J}{kT}\right) + 3\exp\left(\frac{-18J}{kT}\right) + \exp\left(\frac{-20J}{kT}\right)$$

The fitting for the data gave $J = -0.22$ cm^{-1}, $g = 2.02$, and $R = 5.03 \times 10^{-4}$ for **1** and $J = -0.24$ cm^{-1}, $g = 2.00$, and $R = 4.50 \times 10^{-4}$ for **2**, exhibiting weak antiferromagnetic coupling interaction between both the intramolecular Mn(III) sites.

However, the structural difference of **4** from **1**−**3** leads to a variety in magnetic behavior. The increasing of the μ_{eff} value with the lowering of the temperature was observed for complex **4** as shown in Figure 9, indicating total ferromagnetic exchange interaction. To interpret the magnetic behavior of **4**, we used an approximation for the system according to one-dimensional chain structure.[17] Complex **4** can be considered as a uniform chain formed by Mn−(μ-phth)−Mn dinuclear units with classic spin S_{bi} and the magnetic exchange coupling J. The intermolecular magnetic exchange coupling is J'.

On the basis of the assumption of purely isotropic interactions the susceptibility (χ_{bi}) of the dinuclear unit is calculated from eq 2. Then, the S_{bi} can be calculated from

(17) Shen, H.-Y.; Bu, W.-M.; Gao, E.-Q.; Liao, D.-Z.; Jiang, Z.-H.; Yan, S.-P.; Wang, G.-L. *Inorg. Chem.* **2000**, *39*, 396.

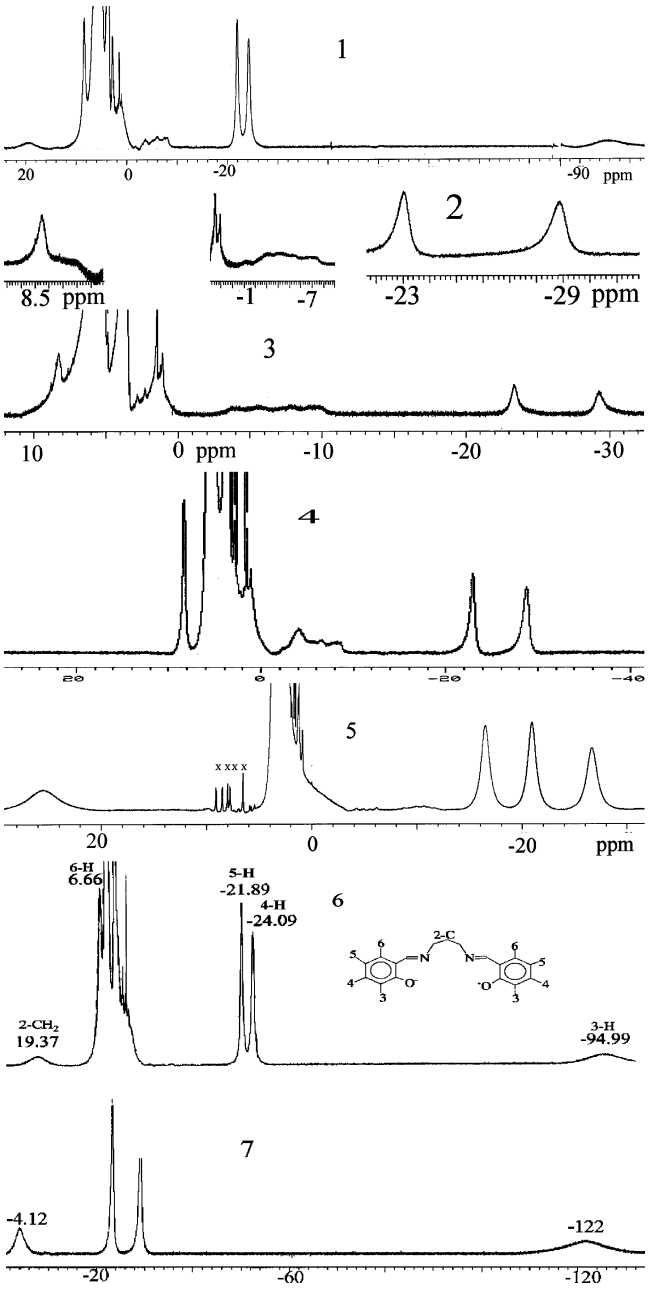

Figure 7. ^{1}H NMR spectra for complexes **1**−**4** and **6**−**7** in CD_3OD and complex **5** in DMSO-d_6. Symbols "×" represent the peaks arising from impurities.

the following eq 3:

$$S_{bi}(S_{bi}+1) = 3k(\chi_{bi}T)/Ng^2\beta^2 \quad (3)$$

The susceptibility (χ) of the one-dimensional chain can be described according to the classical spin model (eq 4) derived by Fisher:[18]

$$\chi = \frac{Ng^2\beta^2 S_{bi}(S_{bi}+1)}{3kT}\left(\frac{1+u}{1-u}\right) \quad (4)$$

where

$$u = \coth\left[\frac{J'S_{bi}(S_{bi}+1)}{kT}\right] - \left[\frac{kT}{J'S_{bi}(S_{bi}+1)}\right]$$

The least-squares fit gave $J = -0.295$ cm^{-1}, $J' = 0.329$ cm^{-1}, $g = 2.02$, and $R = 1.73 \times 10^{-3}$. Similar to other dinuclear complexes with a terephthalato bridge described in this work, complex **4** exhibits weak antiferromagnetic interaction between both the intramolecular Mn sites. It is believed that this magnetic exchange may occur from the long pathway via the benzene ring of the phthalate ligands. Contrasting with the phth pathway, the intermolecular $Mn_2(\mu\text{-}O_{phenolate})_2$ four-member ring may cause the ferromagnetic interaction. As a comparison, the variable temperature susceptibilities of the mononuclear complex (salen)MnCl, which possesses a similar intermolecular $Mn_2(\mu\text{-}O_{phenolate})_2$ correlation,[19] were measured, and the magnetic behavior was examined. An increasing trend of the μ_{eff} value with the lowering of the temperature in the range from 100 to 25 K was observed, showing the similar ferromagnetic exchange interaction to that observed in complex **4**. The relationship of the magnetic properties with the structure of the paramagnetic sites has been discussed in ref 20 for a series of dinuclear Mn(III) compounds involving a similar $Mn_2(\mu\text{-}O)_2$ bridging unit, of which a complex $[Mn(3\text{-}CH_3O\text{-}salen)Cl]_2$[20b] was reported to have $J = 0.33$ cm^{-1} being consistent with the J' value of 0.329 cm^{-1} for complex **4**.

Figure 10 shows the curves of χ_M and μ_{eff} versus T for **6**, revealing the increasing of the μ_{eff} value with the decreasing of the temperature, which is an indication of ferromagnetic exchange interaction between the Mn(III) sites with independent spin $S = 2$. The spin−spin coupling Hamiltonian appropriate for describing the magnetic exchange interaction is presented as the following equation:

$$\hat{H} = -J\hat{S}_{Mn1}\hat{S}_{Mn2} \quad (5)$$

By applying the molar susceptibility expression (eq 2), the susceptibility (χ_{bi}) of the Mn_2(III) unit can be obtained. Then a molecular field approximation[21] was used to treat the interaction between the Mn_2(III) units, giving the susceptibilities of the system.

$$\chi_{system} = \frac{\chi_{bi}}{(1 - zJ'\chi_{bi}/Ng^2\beta^2)} \quad (6)$$

On this basis, the least-squares fitting of the experimental data led to $J = 1.74$ cm^{-1}, $zJ' = -0.125$ cm^{-1}, $g = 1.96$, and $R = 9.03 \times 10^{-5}$, exhibiting that weak ferromagnetic interactions are present in the Mn_2(III) unit. Magnetic interaction approach between both the Mn(III) ions in complex **6** can be usually considered to be either the orbital overlap leading to antiferromagnetic coupling of the Mn(III) ions,[22] or an electron spin polarization[23] leading to a

(18) Fisher, M. E. *Am. J. Phys*. **1964**, *32*, 343.
(19) Pecoraro, V. L.; Butler, W. M. *Acta Crystallogr*. **1986**, *C42*, 1151.
(20) (a) Zhang, Z.-Y.; Brouca-Cabarrecq, C.; Hemmert, C.; Dahan, F.; Tuchagues, J. P. *J. Chem. Soc., Dalton Trans*. **1995**, 1453. (b) Mabad, B.; Luneau, D.; Theil, S.; Dahan, F.; Savariault, J. M.; Tuchagues, J. P. *J. Inorg. Biochem.* **1991**, *43*, 373.
(21) O'Connor, C. J. *Prog. Inorg. Chem*. **1982**, *29*, 203.
(22) Reddy, K. R.; Rajasekharan, M. V.; Tuchagues, J.-P. *Inorg. Chem.* **1998**, *37*, 5978.
(23) Fukita, N.; Ohba, M.; Okawa, H.; Matsuda, K.; Iwamura, H. *Inorg. Chem*. **1998**, *37*, 842.

Table 5. ^{1}H NMR Shifts (ppm) of Related Mn(III) Schiff Base Complexes in CD_3OD

	1	D1	2	3	D3	4	5[a]	6	7
phenolate ring protons	−21.97, −24.26, −95.78	−21.98 −24.23, −96.18	−23.47, −29.31,	−23.42, −29.26	−23.32, −29.14	−23.01, −28.85,	−16.52, −20.92, −26.71	6.66, −21.89, −24.09, −94.99	−4.12, −23.38, −29.16, −122.03,
phth protons	−3.6 to −9.0		−3.5 to −9.4	−3.7 to −10.1		−2.3 to −7.9			
alkylene (or phenylene) backbone protons	19.75	19.70					25.41, 25.99	19.37	

[a] DMSO-d_6 solvent.

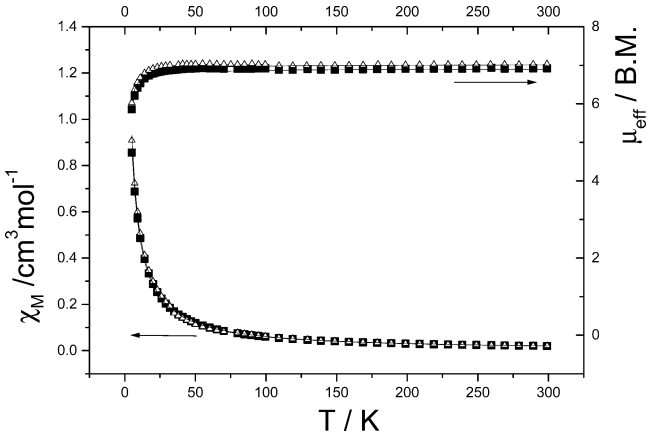

Figure 8. Experimental molar susceptibility (χ_M) and effective magnetic moment (μ_{eff}) of temperature dependence for complexes **1** (■) and **2** (△). The solid lines (—) represent the calculated values.

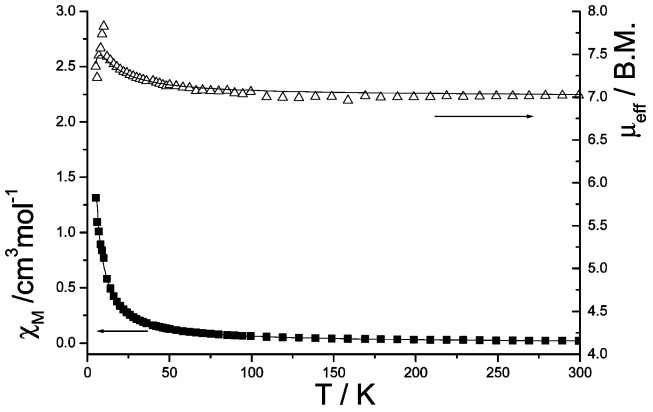

Figure 9. Experimental molar susceptibility (χ_M) and effective magnetic moment (μ_{eff}) of temperature dependence for complex **4**. The solid lines (—) represent the calculated values.

ferromagnetic coupling. Due to Jahn−Teller elongation, only the magnetic orbital d_{z^2} can make a significant contribution to the coupling passing through a Mn−ligand−Na−ligand−Mn bridge to provide a σ-type superexchange pathway. However, due to the long distance and the presence of a diamagnetic sodium ion, this orbital overlap would be obviously weakened and almost ignored. Meanwhile, the mechanism of electron spin polarization may be taken to explain the ferromagnetic coupling between both the Mn(III) ions through the Mn−O−Na−O−Mn linkage.

EPR Spectra and Cyclic Voltammetry of Complex 6. Commonly, the integer spin $S = 2$ Mn(III) ion is very difficult to observe with traditional perpendicular polarization EPR spectroscopy at X-band. The EPR spectra were recorded

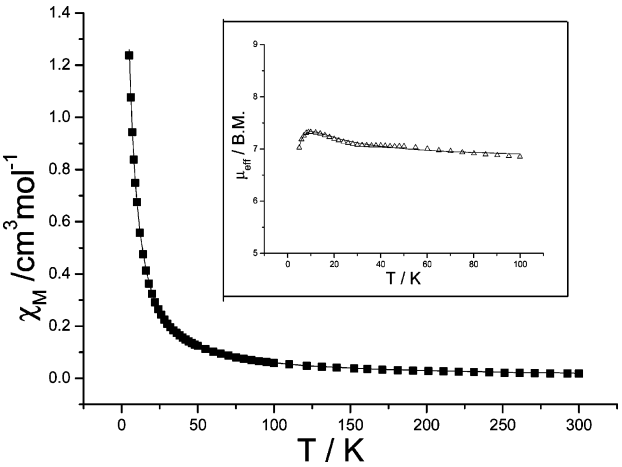

Figure 10. Experimental molar susceptibility (χ_M, 5−300 K) and effective magnetic moment (μ_{eff}, 5−100 K) of temperature dependence for complex **6**.

on a Bruker-ER420 spectrometer at X-band for complexes **1**−**4** and **6** at room temperature and 77 K as solid samples. Complexes **1**−**4** show no EPR signal, while complex **6** reveals signals at $g = 2$. The further characterization was performed by dual mode EPR spectra on a Bruker 380E spectrometer for complex **6**. Figure 11 shows the parallel mode EPR signal composed of six lines with hyperfine resolved structure near $g = 8.2$ and the hyperfine coupling of 47 G.

This characteristic is believed to belong the integer spin $S = 2$ ^{55}Mn(III) ion.[24,25] Moreover, the hyperfine coupling 47 G is very close to the mononuclear Mn(III) salen system reported (46 G).[25] It is proposed that complex **6** contains relatively independent Mn and there was only weak magnetic interaction between the two Mn ions. It is worthwhile to note that the similar signals to that of **6** were also observed in a photooxidazed Mn apo-PSII sample,[24] in which Mn(III) is bound at the high affinity site of the PSII and gave a six-line, $g = 8.2$ signal in parallel mode with hyperfine splitting of 44 G. So, the parallel mode EPR signals indicate the existence of the Mn(III) site with $S = 2$ in complex **6** and show the potential correlation between complex **6** and the photooxidation intermediate of the PSII.

The perpendicular mode EPR spectrum of **6** shown in Figure 12 contains a six-line signal at $g = 2.0$ and a six-peak signal at $g = 8.1$. Both the signals appearing at high

(24) Campbell, K. A.; Lashley, M. R.; Wyatt, J. K.; Nantz, M. H.; Britt, R. D. *J. Am. Chem. Soc.* **2001**, *123*, 5710.
(25) Campbell, K. A.; Force, D. A.; Nixon, P. J.; Dole, F.; Diner, B. A.; Britt, R. D. *J. Am. Chem. Soc.* **2000**, *122*, 3754.

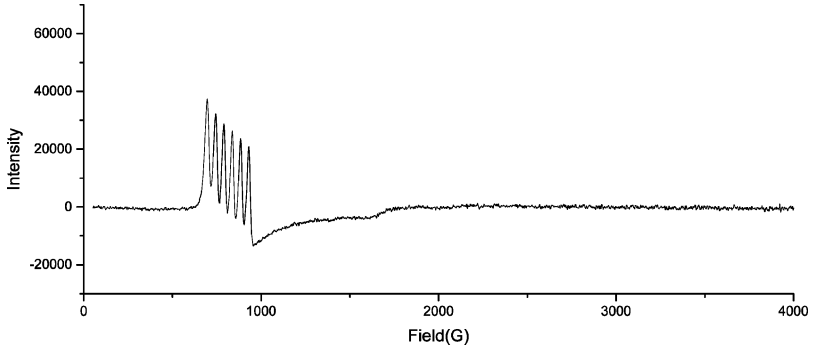

Figure 11. Parallel mode EPR of **6** with six-line signal at $g = 8.2$. Measurement conditions: 10 K, microwave power 2 mW, microwave frequency 9.35 GHz, modulation amplitude 100 kHz, modulation amplitude 12 G, scan number 8.

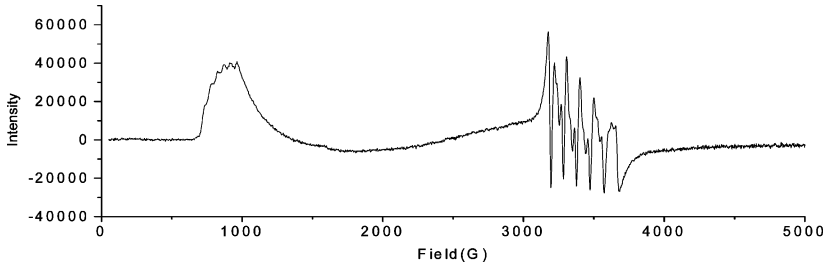

Figure 12. Perpendicular mode EPR signals at $g = 8.1$ and 2.0. Measurement conditions are the same to those used in Figure 11 except the temperature is 4 K.

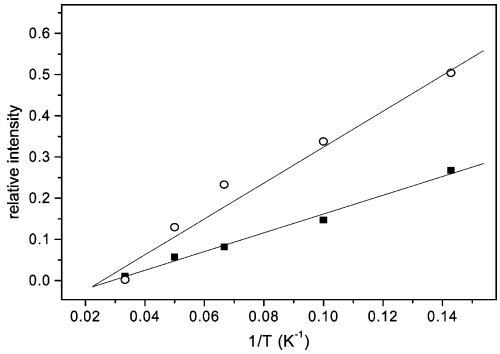

Figure 13. Temperature dependence of the relative signal intensities (versus the signal intensity at 4 K) at $g = 2.0$ (○) and 8.1 (■) in the range 7−30 K.

and low magnetic field, respectively, were generally associated with the Mn(II) species with spin $S = {}^5/_2$. However, a $g = 8.1$ perpendicular mode EPR signal from a Mn(III) salen species was also observed recently,[25] confirming the contribution of the Mn(III) salpn species to this signal. The temperature dependence of both the signal intensities at 7−30 K and the different slopes (Figure 13) of the two curves seem to suggest the existence of an independent Mn(II) site ($S = {}^5/_2$). However, the structural, ^{1}H NMR, and magnetic data do not support the presence of the Mn(II) ions in the complex. It is better to consider that the presence of a paramagnetic Mn(II) impurity might be responsible for the six-line signal at $g = 2.0$ and might explain the described EPR behavior of this complex.

Cyclic voltammetry of **6** in CH_3OH reveals only one quasireversible redox pair at −0.29 V/−0.12 V in a scan range between +1.0 and −1.2 V, implying more simple redox chemistry than that of $[C_2H_9O_2][Mn_2Na(2\text{-HO-salpn})_2(OAc)_4]$.[11] This could be assigned as the quasireversible redox of $Mn(III)_2/Mn(II)Mn(III)$ in **6**, and the reversibility can be seen as an indication of the intactness of the complex backbone in solution.

Mixed metal dinuclear manganese complex **6** has been characterized by different methods since the complex may provide insight toward the structure of the OEC in PSII, especially the possible mode of calcium binding to the Mn sites in the OEC. Our further research will focus on the preparation and characterization of bimetallic $Mn_{2-4}Ca$ cluster, which may provide access to the effective artificial oxygen-evolving system.

Acknowledgment. This work was supported by State Key Basic Research and Development Plan of China (G1998010100) and NNSFC (No. 30170229) and Expert Project of Key Basic Research from Ministry of Science and Technology.

Supporting Information Available: X-ray crystallographic files in CIF format, and listings of crystallographic data, atomic coordinates and *B* values, bond lengths and angles, and anisotropic thermal parameters for complexes **1**−**6**, **D1**, and **D3**. IR spectral data. This material is available free of charge via the Internet at http://pubs.acs.org.

IC025944Z